

Direct electrooxidation of 3-methyl-4-nitrophenol (MNP) at carbon fiber microelectrode (CFME)

Yibor Fabrice Roland Bako¹, Issa Tapsoba^{1,*}, Maxime Pontie², Mohamed Lyamine Chelaghmia³

¹ Laboratoire de Chimie Analytique Environnementale et Bio-Organique, Département de Chimie, Université Ouaga I, 03 BP 7021 Ouagadougou 03, Burkina Faso

² Université d'Angers, SFR Santé, Laboratoire GEIHP EA 3142, Institut de Biologie en Santé, PBH-IRIS, CHU, 4 Rue Larrey, 49933 Angers Cedex 9, France

³ Département de Génie des Procédés, Laboratoire d'Analyses Industrielles et Génie des Matériaux, Université 8 Mai 1945 Guelma, BP 401, Guelma, Algeria

*E-mail: issa.tapsoba@gmail.com, issa.tapsoba@univ-ouaga.bf

Received: 23 April 2018 / Accepted: 6 June 2018 / Published: 5 July 2018

The direct electro-oxidation of 3-methyl-4-nitrophenol (MNP), main by-product of the insecticide fenitrothion (FT), both endocrine disruptors, leads to carbon electrode passivation due to electrodeposition of polyphenol on electrode surface. To overcome this problem usual electrochemical cleanings, help the users to treat the electrode surface. Due to the little diameter of the carbon fiber, this solution is unusable for a carbon fiber microelectrode (CFME). We proposed presently, for the first time on a CFME, an original anti-passivating strategy based on the optimization of the initial oxidation potential (-1.2 V vs 0 V/ Ag/AgCl) with or without a CFME modification by a film of nickel tetrasulfonated phthalocyanine (p-NiTSPc) electrodeposited in alkaline solution. This original strategy was studied in the light of electrode sensitivity dedicated to MNP analysis.

Keywords: CFME; MNP; Electrochemical cleaning, anti-passivation, initial potential; p-NiTSPc film

1. INTRODUCTION

Organophosphorus (OPs) compounds are pesticides widely used for insect control to improve yields in agriculture production [1–4]. Thus, according to the United Nations Organization statistics Food and Agriculture Organization (FAO), in Burkina Faso over 500 tons of pesticides are used each year since 2010 [5]. Among them, fenitrothion (FT), an organophosphate insecticide is widely used in cotton crop in the north of this country. FT like other organophosphates, acts by inhibiting the acetylcholinesterase and then disrupting the nerve impulses transmission [2,6,7]. FT has the property of fast degradation and generally low accumulation in the environment [8]. 3-methyl-4-nitrophenol

(MNP) is the main by-product of FT degradation especially in soil [8,9] and is very persistent in environment, particularly in water. MNP is highly toxic because it is an endocrine disruptor [4,6,10–12] and then may cause adverse in the biological systems. Therefore, due to their high potential health and environmental impacts, it is necessary to develop analytical methods for determination of these pollutants in the environment. Although different analytical methods have been used for the determination of OPs [3,4,6,8,13–18], electroanalytical techniques are a more attractive choice, due to their simple operation, high sensitivity, and good selectivity [8,13,15–17,19–23]. Several works were reported on the use of ultramicroelectrodes (UMEs) in electroanalytical methods for OPs pesticides and/or their metabolites quantification [13,22,23]. UMEs are widely used because their small size gives them very attractive properties such as: a reduced ohmic potential drop, a decreased time constant, a fast establishment of steady-state signals, an increased signal-to-noise ratio, a restricted volumes and a short-time analysis in solutions of high resistance [24,25]. Furthermore, the direct oxidation of organic micropollutants phenol-likes, i.e. acetaminophen, *p*-aminophenol, hydroquinone or nitrophenol leads to the electrode surface a dramatic polyphenol film formation blocking repetition of the analysis by passivation phenomena [20,26,27].

In this paper, we report an original work dedicated to a novel anti-passivating procedure for the direct oxidation of MNP, a very persistent endocrine disruptor in polluted water resources (1 to 3 years), studying the optimal initial potential for unmodified and modified CFME surface by an electrodeposited film of Ni-phthalocyanine, in comparison to a usual electrochemical cleaning.

2. EXPERIMENTAL

2.1. Reagents and materials

Carbon fibers (12 μm diameter, 5 mm length) were purchased from Cytec Engineered Materials (West Paterson, NJ, USA) and used for CFME elaboration. MNP, nickel tetrasulfonated phthalocyanine (NiTSPc), potassium ferrocyanide ($\text{K}_4\text{Fe}(\text{CN})_6$), Na_2HPO_4 and NaH_2PO_4 were purchased from Sigma Aldrich. Fenitrothion was containing on formulation Fenical SL by Saphyto Arysta Life. All reagents were used without purification and all solutions were prepared with deionized water (pH 6.5, conductivity $< 0.1 \mu\text{S}/\text{cm}$ and DOC $< 0.1 \text{ mg}/\text{l}$).

2.2. Apparatus

All electrochemical experiments were performed with a potentiostat PG581 (Uniscan Instrument) controlled by a computer using UiEChem program, both purchased by Biologic (France). A conventional three electrodes electrochemical cell was used with $\text{Ag}/\text{AgCl}/\text{Cl}^-$ as the reference electrode, CFME or CFME modified with p-NiTSPc denoted CFME/p-NiTSPc as working electrode and platinum wire as counter electrode.

2.3. CFME modification by p-NiTSPc

Prior to modification the working electrode was cleaned electrochemically in 0.5 M H₂SO₄ with ethanol (1:1) by performing 10 voltammetric cycles at the scan rate 50 mV/s. After cleaning, the working electrode was modified following the method already reported [23]. Shortly: Electrodeposition is first initiated by performing five voltammetric cycles in aqueous solution containing 0.1 M NaOH with the potential range of 0 to 1.3 V at a scan rate of 100 mV/s, after that the p-NiTSPc is electrodeposited by performing 50 voltammetric cycles in 2 mM NiTSPc aqueous solution prepared in 0.1 M NaOH, in the same potential range. The presence of p-NiTSPc on the modified CFME was confirmed by performing one voltammetric cycle in 0.1 M NaOH from 0.4 V to 0.7 V at a scan rate of 100 mV/s. Figure 1 showed the obtained voltammograms respectively for the electrodeposition of p-NiTSPc on CFME and the electrochemical revelation of modified CFME/p-NiTSPc. The p-NiTSPc film thickness was evaluated from the last cyclic voltammogram of p-NiTSPc electrodeposition. Under these experimental conditions, the p-NiTSPc film electrodeposited present a recovering of approximately 2×10^{-8} mol/cm² determined from the integration of the oxidation peak, which correspond to a film thickness of 290 nm, as previously reported [28].

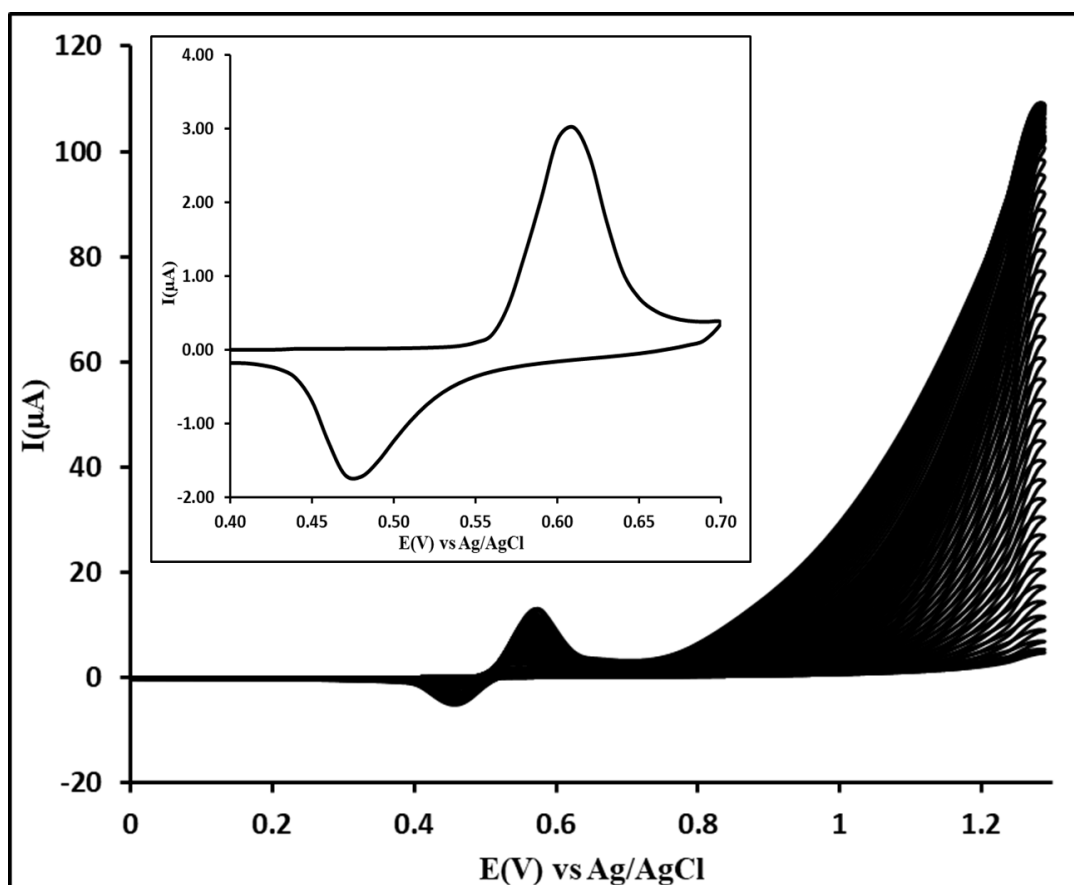


Figure 1. 50 successive cyclic voltammograms of CFME in a 0.1 M NaOH aqueous solution containing 2mM of NiTSPc at the potential scan rate of 100 mV/s and in insert 1 cyclic voltammogram of CFME/p-NiTSPc in a 0.1 M NaOH aqueous solution at the potential scan rate of 100 mV/s.

2.4. Evaluation of sensors sensitivity decreasing

In order to evaluate the performance decreasing of sensors, the ion ferrocyanide (denoted Fe^{II}) has been chosen as a probe, as usually in electrochemistry. It consists to calculate the relative variation of Fe^{II} oxidation peak ΔI after using sensors for MNP direct oxidation in 5 successive cycles. The formula used is:

$$\Delta I(\%) = \frac{I_0 - I}{I_0} \times 100$$

with I_0 the Fe^{II} oxidation peak intensity before the use of sensor for MNP analysis and I the Fe^{II} oxidation peak intensity after the use of the same sensor for MNP analysis. The same formula was also used to estimate the MNP oxidation peak intensity variations due to passivation.

To estimate the real surface area of the electrode, CFME and CFME/p-NiTSPc were used to record cyclic voltammogram of a 5 mM Fe^{II} solution in 0.1 M PBS (pH 6.5). Then, the real surface area can be calculated using the Randles-Sevcik equation [29]:

$$I_p = 2.69 \times 10^5 n^{3/2} \nu^{1/2} D^{1/2} AC$$

where I_p is the peak intensity of the analyte Fe^{II}, n is the number of electrons transferred, ν is the potential scan rate in V/s, A is the area of the electrode in cm², C is the concentration of the analyte in mol/cm³ and D in cm²/s is the diffusion coefficient of Fe^{II} which has been reported to be 7.6×10^{-6} cm²/s.

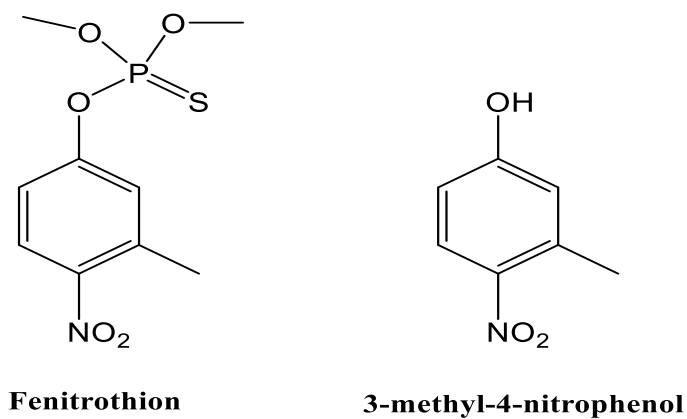
2.5. Scanning Electronic Microscopy (SEM) and Atomic Force Microscopy (AFM) images of the CFME tested

SEM experiments were performed on CFME and CFME/p-NiTSPc, using a JEOL type JSM-6301F (SCIAM, Angers university). Images obtained were from secondary electrons under 3-5 keV with magnifications situated between 3000 and 5000. Figure 2 shows the surface morphology of the CFME and CFME/p-NiTSPc. AFM was used to observe the topography of unmodified and modified CFMEs surfaces. The microscope used is a VEECO Nanoscope III and the images were obtained in contact mode in the air with a scan rate of 1.5 Hz, a pressing force of 10 nN and other an area of $2 \times 2 \mu\text{m}^2$ analysis. Our image analysis consisted in determining the average roughness (Ra) of the different surfaces analysed.

3. RESULTS AND DISCUSSION

3.1. Comparison of voltammetric behaviour of FT and MNP on CFME

A comparison of the molecular structure of FT and MNP (scheme 1) shows that these two organic molecules are similar due to the same (-NO₂ functional groups), we opted for a direct oxidation analysis for MNP detection in presence of FT because the MNP possesses also a phenol function which permit a selectivity in a mixture of MNP and FT solution.



Scheme 1. Chemical structure of Fenitrothion and 3-methyl-4-nitrophenol

Cyclic voltammograms of FT and MNP in PBS at the scan rate 100 mV/s using a CFME are presented on Figure 2.

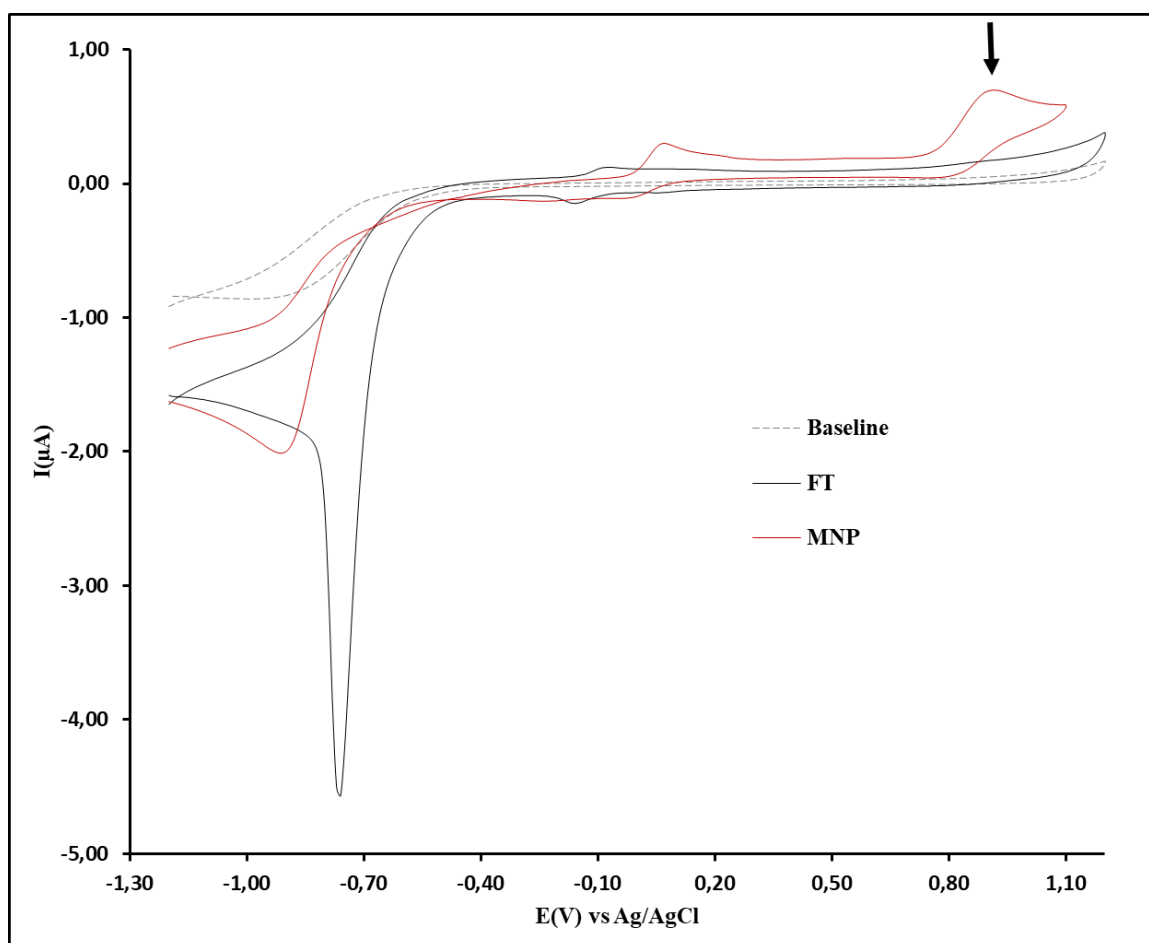
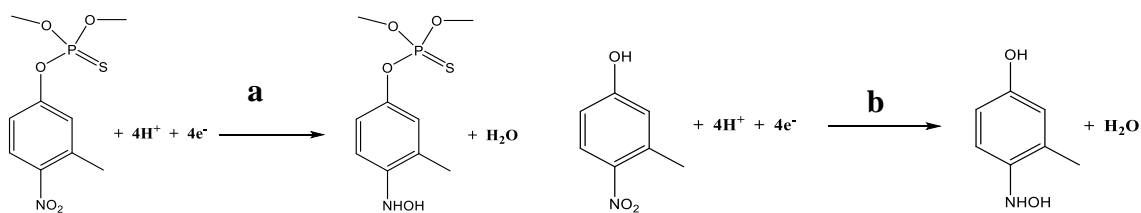


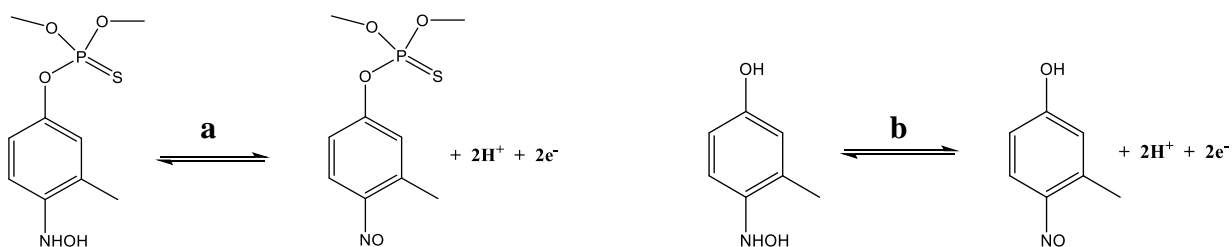
Figure 2. Cyclic voltammogram in 0.1 M PBS (pH 6.5) on unmodified CFME at the scan rate 100 mV/s with 1 min of electrolysis time at the initial potential -1.2 V of 30 mg/L: (grey) FT and (red) MNP.

It can be seen from figure 2 that FT and MNP present an irreversible reduction peak situated at -0.79 V and -0.90 V, respectively. According to the literature these peaks are due to the reduction of nitro group into hydroxylamine [2,23] and could be described by Scheme 2.



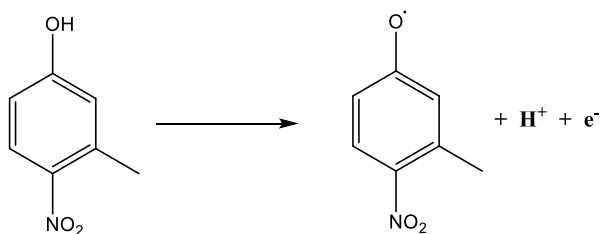
Scheme 2. Direct redox reduction of (a) FT and (b) MNP.

We also observed in Figure 2, two redox peaks at -0.01V and -0.19V for FT and at 0.07V and -0.02V for MNP which correspond to the oxidation of the hydroxylamine into nitroso group and the reduction of nitroso into hydroxylamine group as reported previously [23]. These peaks could be described by the Scheme 3.



Scheme 3. Indirect oxidation reaction of (a) FT and (b) MNP.

Furthermore, it can be seen on Figure 2 an irreversible anodic peak at +0.92V due to the direct oxidation of phenol group of MNP, as reported elsewhere [23,30,31] and this peak could be described by Scheme 4:



Scheme 4. Direct oxidation reaction of MNP

The irreversibility of this peak is explained by the presence of a chemical reaction of deactivation of the radical cation formed after the charge transfer. This reaction could be a deprotonation or polymerization reaction of the radical cation.

Nevertheless, the presence of this peak of a direct oxidation of MNP is very interesting because the direct oxidation should be a good way for a selective analysis of MNP in presence of FT. For the rest of this work we will be focused on this peak.

3.2. SEM/AFM results

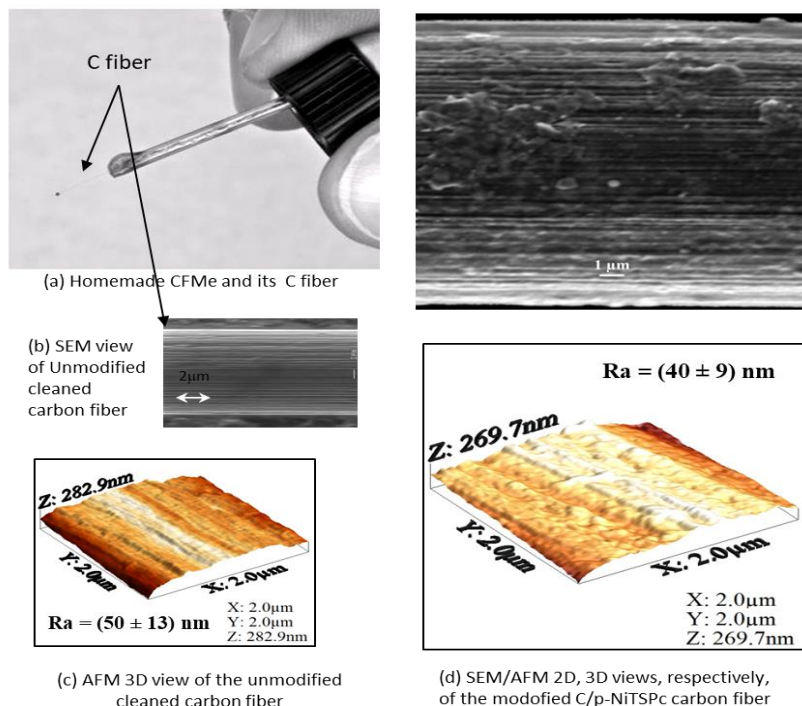


Figure 3. SEM/AFM images of CFMEs: (a) macroscopic view of the homemade CFME and the carbon fiber; (b) unmodified cleaned carbon fiber; (c) AFM 3D view of the unmodified CFME; (d) SEM/AFM images of the modified CFME/p-NiTSPc after 50 cycles of NiTSPc electrodeposition in alkaline solution (NaOH 0.1 M, NiTSPc 2 mM, scan rate 100 mV/s).

The Figure 3 show macroscopic and microscopic views of the CFME studied. Fig. 3b shows the clean carbon fiber and permit to check its fiber diameter at 12 μm, as on the Fig. 3c we observe the topography of the unmodified CFME. Its average roughness is 50 nm. In the Fig. 3d we compared morphology and topography analysis of the modified CFME, its roughness was determined at 40 nm, very similar to the unmodified.

3.3. Direct oxidation of MNP and CFME passivation illustration

It is well known that oxidation of phenol derivatives leads to the formation of polymeric film on the electrode surface and cause electrode passivation [26,27,32–34].

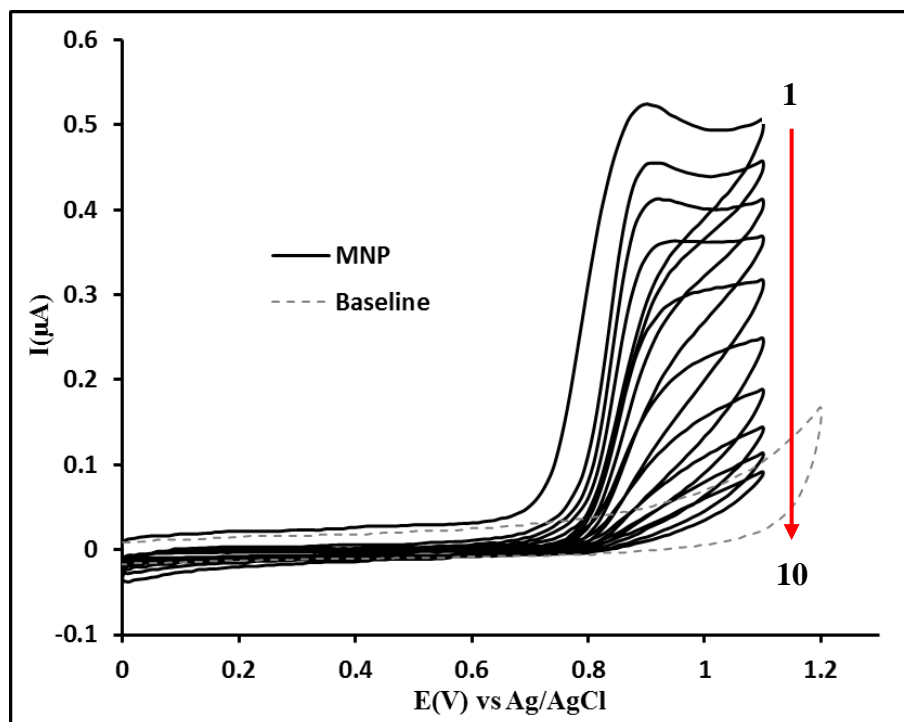
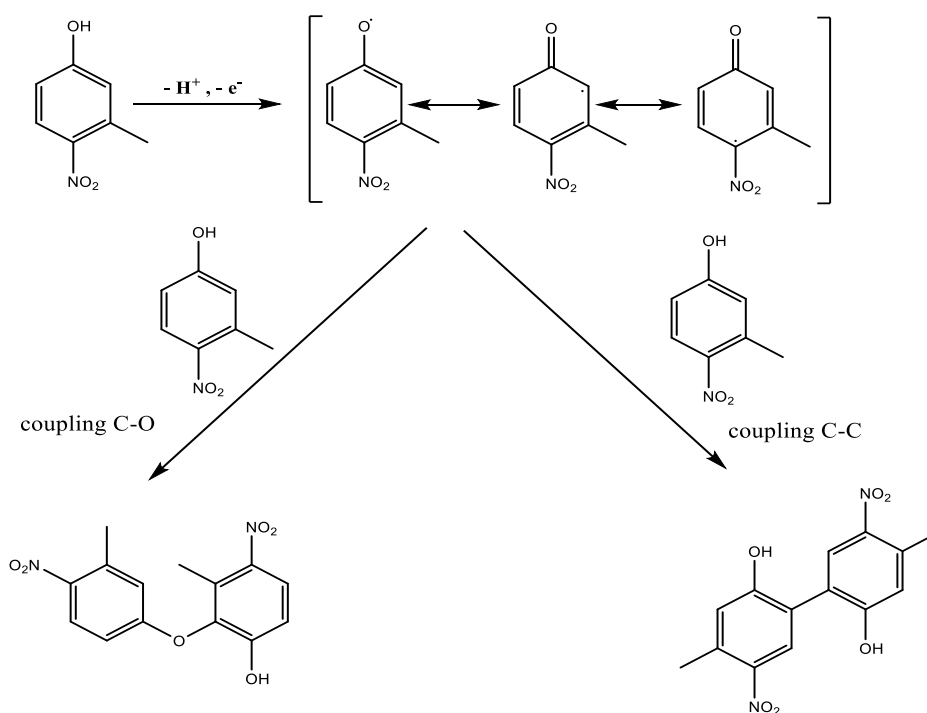


Figure 4. 10 successive cyclic voltammograms of MNP at 30 mg/L in PBS (pH 7, 0.1 M) on CFME with a potential scanning rate of 50 mV/s.

It can be seen on the Figure 4 that the oxidation peak is decreasing with increasing scan number. This electrode passivation could be explained by the electrodeposition of polyphenol film, as illustrated on GCE elsewhere [27]. The formation of this film is started by a dimerization reaction (two ways) from a radical electrogenerated, as illustrated by Scheme 5.



Scheme 5. MNP oxidation and dimerization pathways [26]

In the present study we purpose to develop a new strategy to prevent or reduce this phenomenon and also to improve CFME sensor sustainability, limiting the apparition of this passivation phenomenon.

3.4. Removal of MNP polymer film by electrochemical cleaning

Cyclic voltammograms of Fe^{II} on CFME before and after electrode passivation in five successive cycles in 5 mg/L of MNP, and also after electrochemical cleaning of passivated electrode are showed in Figure 5.

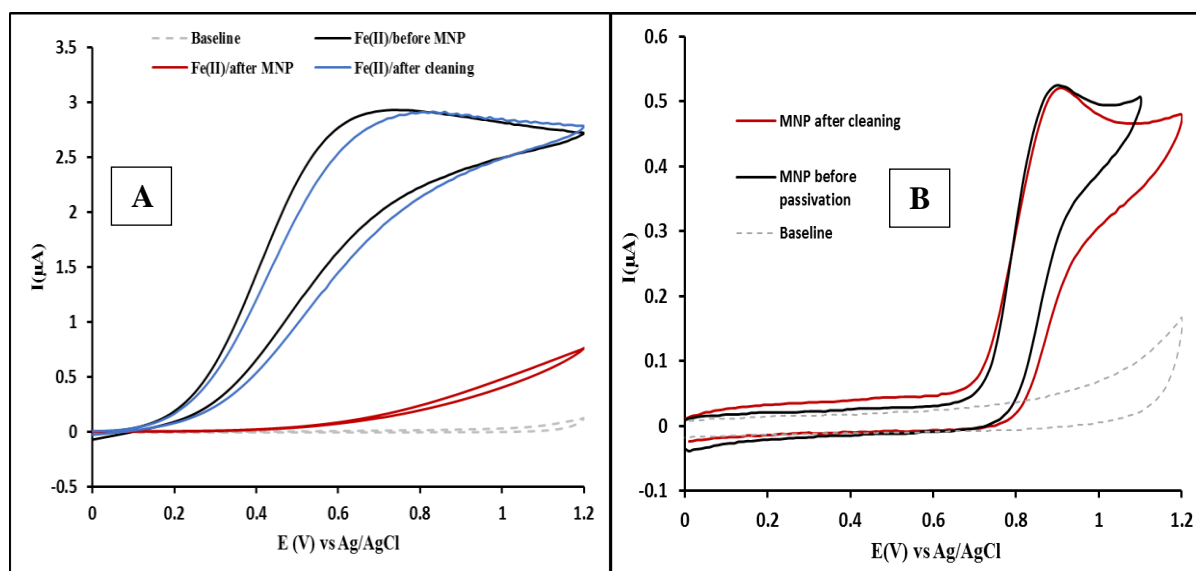


Figure 5. Cyclic voltammograms of (A) $\text{Fe}(\text{CN})_6^{4-}$ 5 mM at the scan rate 100 mV/s on CFME before (black) and after (red) electrode passivation and after electrochemical cleaning of passivated electrode (blue) with 10 successive cycles in $(\text{H}_2\text{SO}_4$ 0,5M/EtOH) (1:1, v/v).

One can see on the figure 5A a total disappearance of Fe^{II} oxidation peak using CFME for MNP oxidation. This result confirms the modification of the electrode surface due to a polymeric film deposition of polyphenol. Nevertheless, we observe always on Figure 5A that the oxidation peak of Fe^{II} reappeared with a recovery of 99 % of the initial intensity after electrochemical cleaning of CFME (2.93 μA initially and 2.91 μA after cleaning). We can see on Figure 5B similar result after electrochemical cleaning of passivated CFME (0.53 μA initially and 0.52 μA after cleaning). These results indicate that it is possible to regenerate CFME by electrochemical cleaning after passivation and then recover its sensitivity by this electrochemical cleaning.

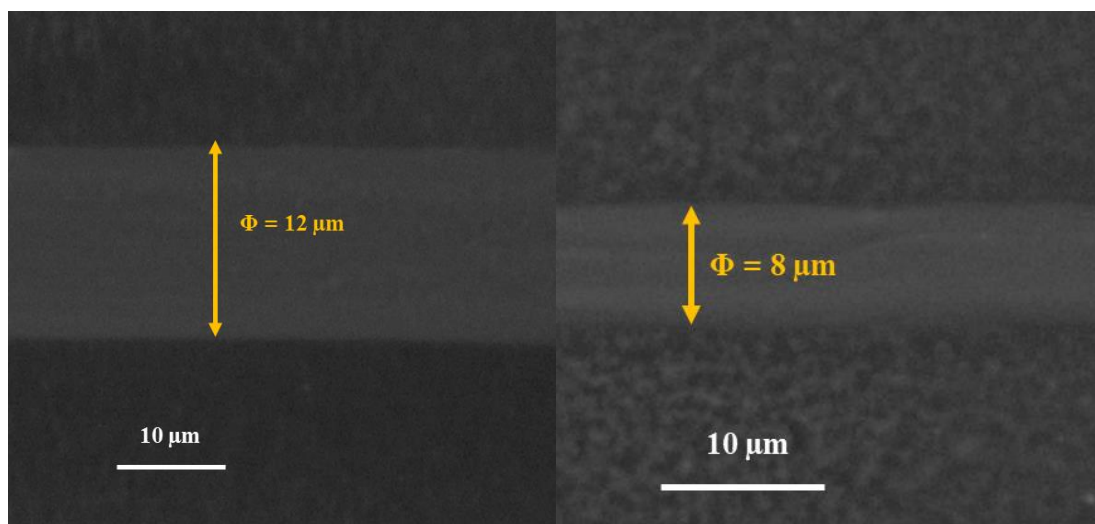
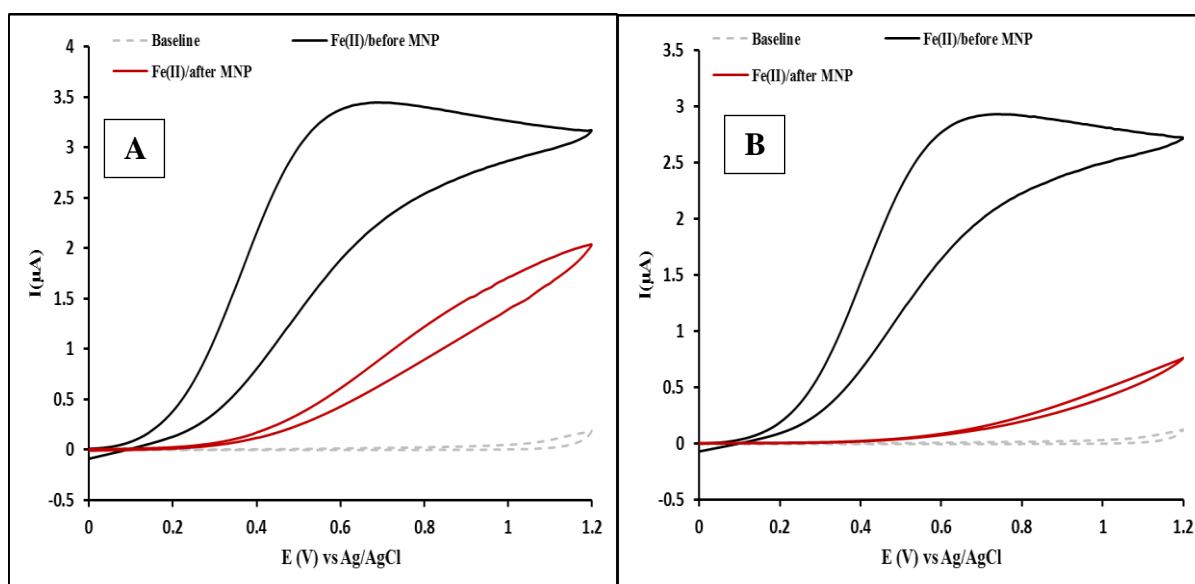


Figure 6. SEM images of carbon fibers: (a) before electrochemical cleaning and (b) after electrochemical cleaning.

Thus, SEM analysis of a carbon fiber before and after an electrochemical cleaning (see Fig. 6) shows a decrease in the diameter of the carbon fiber of $4 \mu\text{m}$ (from 12 to $8 \mu\text{m}$) and that could reduce dramatically the diameter of CFME, weaken it and then limit its lifetime. This result was well known in electrochemical cleaning [22]. If such cleaning is applied successively after each analysis the fiber will be broken quickly. To limit that we explored other possibilities of MNP analysis based on direct oxidation peak in order to restrict considerably the use of electrochemical cleaning.

3.5. Evaluation of the potential range analysis effect on CFME passivation

Figures 7A and 7B show cyclic voltammograms of Fe^{II} obtained before and after using CFME for the oxidation of MNP in five successive cycles in two different potential ranges.



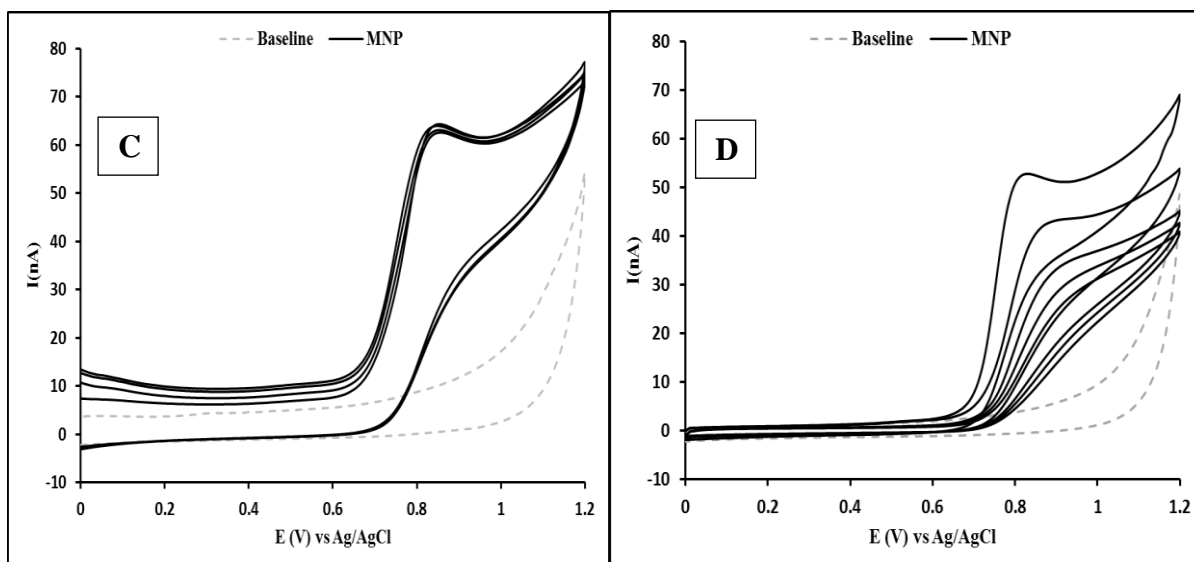


Figure 7. Cyclic voltammograms of $\text{Fe}(\text{CN})_6^{4-}$ 5 mM on CFME before and after analysis of MNP from -1.2 V to 1.2 V (A) and from 0 V to 1.2 V (B) ;5 successive cyclic voltammograms of MNP 5mg/L on CFME from -1.2 V to 1.2 V (C) and from 0V to 1.2 V (D).

It can be seen on these figures 7A and 7B a drastic decrease of oxidation peak intensity of Fe^{II} after using CFME for MNP oxidation. These results confirm the passivation of the electrode. Furthermore, electrode passivation appeared less important when analysis of MNP is performed from -1.2 V to 1.2 V (Fig. 7A) in comparison with 0 V to 1.2 V (Fig. 7B). Indeed, ΔI of Fe^{II} oxidation peak intensity are 76% and 95% for both potential range studied, -1.2 V to 1.2 V and 0 V to 1.2 V (see table 1), respectively.

Table 1. Potential, intensity and relative intensity variation of Fe^{II} oxidation peak before and after using sensors for MNP analysis in direct oxidation.

Sensors	Potential range of MNP analysis	Fe^{II}		
		I_0 (μA)	I (μA)	ΔI (%)
CFME	-1.2 V to 1.2 V	3.45	0.83	76
	0 V to 1.2 V	2.93	0.15	95
CFME/p-NiTSPc	-1.2 V to 1.2 V	3.55	3.25	8
	0 V to 1.2 V	5.21	4.78	8

Table 2. Potential, intensity and relation variation intensity of MNP oxidation peak when analysis is performed in the potential ranges -1.2 V to 1.2 V and 0 V to 1.2 V.

Sensors	Potential range of MNP analysis	MNP		
		I_0 (nA)	I (nA)	ΔI (%)
CFME	-1.2 V to 1.2 V	62.40	54.00	13
	0 V to 1.2 V	50.63	13.13	74
CFME/p-NiTSPc	-1.2 V to 1.2 V	72.00	60.00	17
	0 V to 1.2 V	59.50	53.63	10

In addition, the analysis of MNP in several successive voltammetric cycles shows that there is almost no decrease of peak intensity for an initial potential $E_i = -1.2$ V (Fig. 7C) while a drastic decrease of this peak intensity is observed for an initial potential $E_i = 0$ V (Fig. 7D). The estimation of the relative variations of MNP peak intensity is presented on table 2.

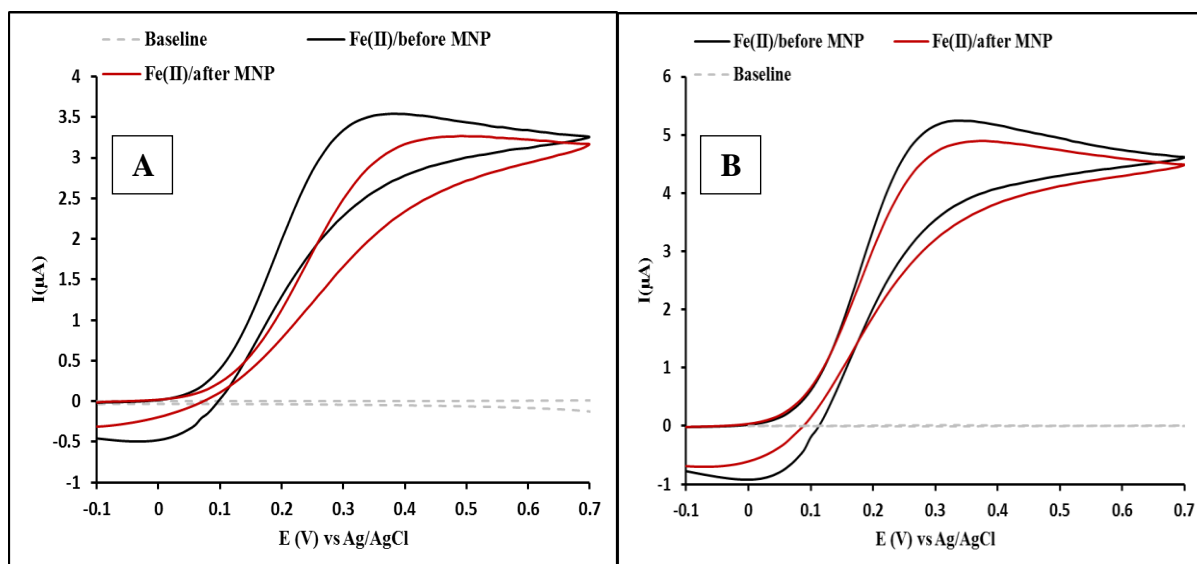
These results are in agreement with those reported by Pontié on *p*-nitrophenol with a GCE electrode [20]. In fact, starting analysis at a low potential lead to the formation of a soluble monomer 3-methyl *p*-aminophenol, limiting the radical cation formation. According to the literature, *p*-NiTSPc can be used to prevent passivation of sensor used for electrooxidation of phenol derivatives [35]. Presently, if the initial potential influence passivation formation and the initial potential of -1.2 V is the best condition; in presence of *p*-NiTSPc the initial potential of -1.2 is not the optimum potential, as seen in the Table 2. Finally, for the modified CFME the optimum initial potential is 0 V.

Then, we investigated the effect of NiTSPc on the passivation of CFME by electrooxidation of MNP.

3.6. Evaluation of the effect of *p*-NiTSPc film on CFME passivation

Figures 8A and 8B show voltammograms of Fe^{II} before and after using CFME/*p*-NiTSPc for MNP direct oxidation. It can be seen a decreasing of Fe^{II} oxidation peak relatively to the peak before MNP analysis.

This decreasing is about 8 % (see table 1) when MNP analysis is performed in the two potential ranges 0V to 1.2V and -1.2 V to 1.2 V. Furthermore, we can see on Figures 8C and 8D (see also table 2) that there is almost very low decrease in the peak intensity of MNP when five successive cycles of MNP were performed on modified CFME/*p*-NiTSPc independently of the initial potential choice, with a little difference observed between 0 V and -1.2 V for the initial potential, with 10% and 17% of peak extinction, respectively.



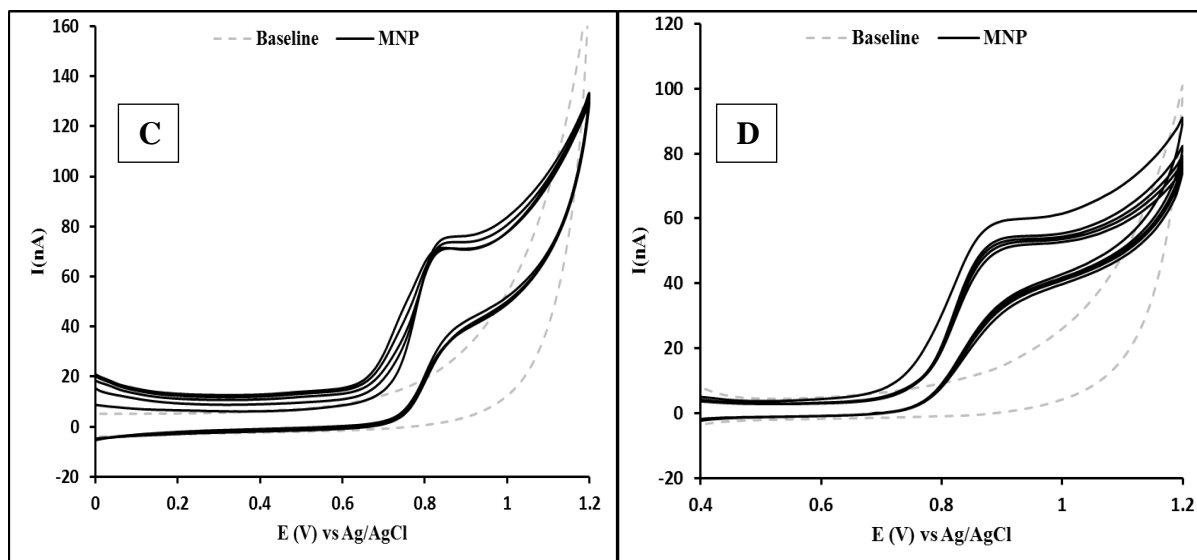


Figure 8. Cyclic voltammograms of $\text{Fe}(\text{CN})_6^{4-}$ 5 mM on CFME/p-NiTSPc before and after analysis of MNP in potential range -1.2 V to 1.2 V (A) and 0V to 1.2 V (B) ;5 successive cyclic voltammograms of MNP 5mg/L on CFME at potential range -1.2 V to 1.2 V (C) and 0 V to 1.2 V (D).

Comparatively to unmodified CFME results, the decreasing of CFME/p-NiTSPc sensitivity is less important and can be attributed to p-NiTSPc film through its particular O-Ni-O bridges architecture $\beta\text{-Ni}(\text{OH})_2$ as previously reported in similar case and which stabilize the electrode surface [36]. Then p-NiTSPc film could enable the prevention of CFME passivation and then improve its sustainability for successive analysis.

3.7. Study of electrochemical behaviour of MNP on CFME/p-NiTSPc

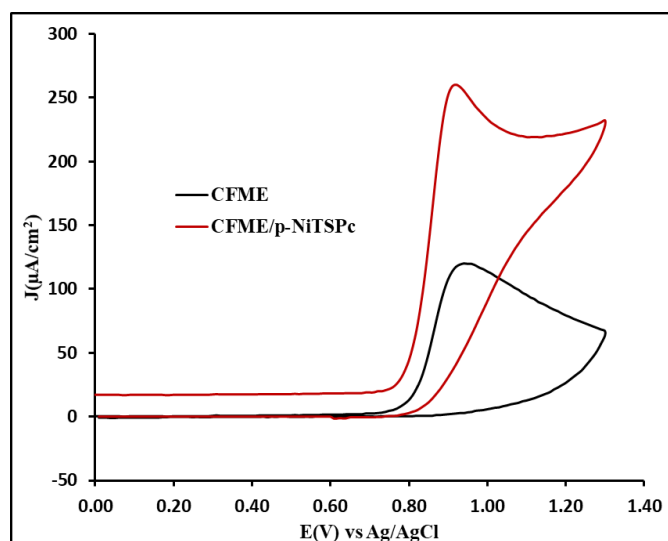


Figure 9. Cyclic voltammograms of MNP 70 mg/L in PBS (pH = 7, 0.1 M) obtained using naked CFME (black curve) and p-NiTSPc modified CFME (red curve) at the scan rate 100 mV/s. Initial potential: 0 V.

Figure 9 shows cyclic voltammogram of the direct electrooxidation of MNP obtained using unmodified CFME and modified CFME/p-NiTSPc.

We can observe on this Figure 9 the increase of the oxidation current density of MNP after CFME modification by p-NiTSPc. However, the oxidation peak potential of MNP remains constant. This result suggested that the increase of oxidation peak signal would not be due to an electrocatalytic effect but rather to an enhancement of the real surface area of CFME. This behaviour was already observed on GCE for 2,4-dichlorophenol and other polychlorinated phenols [27].

The real surface areas of CFME and CFME/p-NiTSPc were investigated by cyclic voltammetry using 5 mM Fe^{II} solution and the results are shown in Figure 10. The real surface areas were calculated by mean of the Randles-Sevcik equation. The obtained real surfaces were $2.544 \times 10^{-3} \text{ cm}^2$ and $2.958 \times 10^{-3} \text{ cm}^2$ for unmodified and modified CFMEs studied respectively, as the geometrical area calculated was $1.877 \times 10^{-3} \text{ cm}^2$.

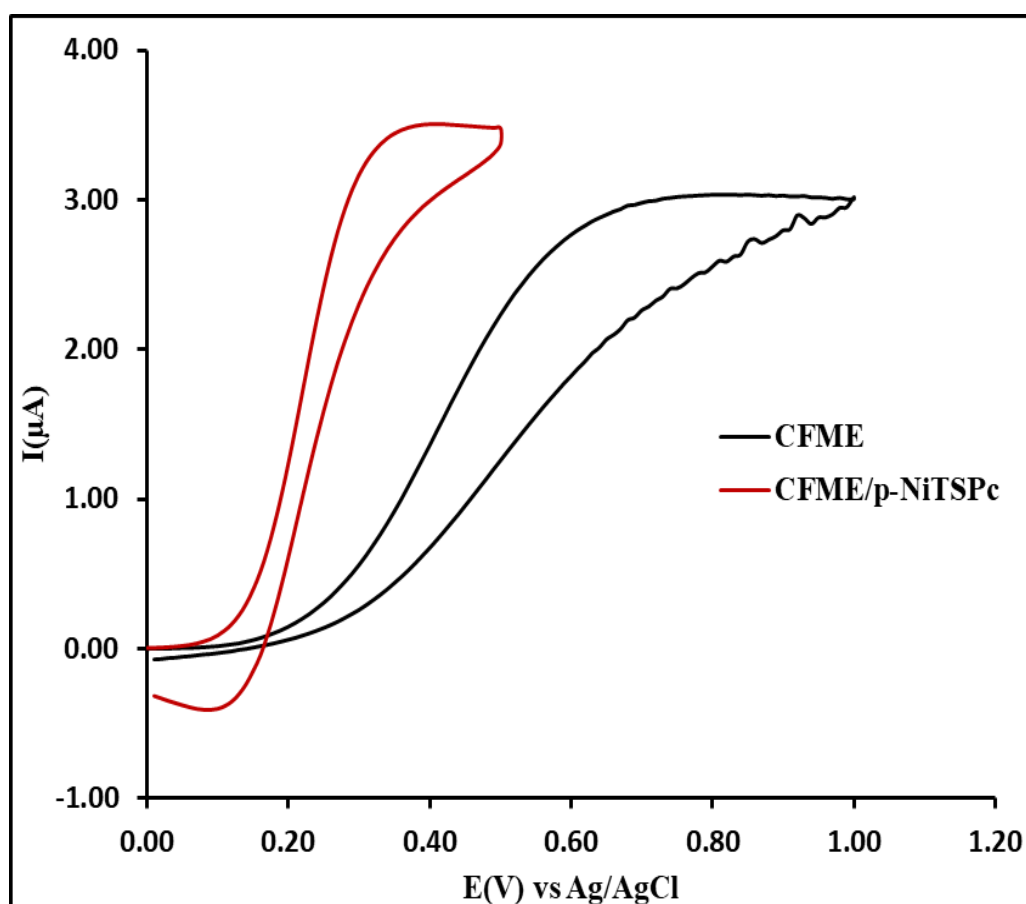


Figure 10. Cyclic voltammograms of 5 mM Fe^{II} in PBS at (black curve) naked CFME and at (red curve) CFME/p-NiTSPc. Potential scan rate: 100 mV/s.

According to Mbokou et al [37], one can determine physical and chemical effect by calculating the ratio of peak intensity and of real surface area obtained with modified CFME, in relation to the naked CFME.

Table 3 presents the ratios of real surface areas and peak intensities of MNP when cyclic voltammogram of 70 mg/L MNP is recorded.

Table 3. Ratios of real surface areas and peak intensities of 70 mg/L MNP.

Electrodes	Ratio of I_p with modified electrode versus CFME	Ratio of real surface area of modified electrode versus CFME	Chemical effect (hydrophilic character of p-NiTSPc)
CFME/p-NiTSPc	2.290	1.163 (50%)	1.127 (50%)

The analysis of this table shows that p-NiTSPc enhance the sensitivity of CFME by two ways: physical effect due to an increase of the real surface area and chemical effect owing to the hydrophilization of electrode surface, presently in the ratio of 50/50.

4. CONCLUSION

We propose an anti-passivation strategy for MNP direct oxidation analysis for the first time on a CFME. Indeed, a good choice of potential range work (-1.2V to 1.2V) for unmodified CFME and (0V to 1.2V) for modified p-NiTSPc CFME could allow to reduce considerably electrode passivation and enhance its durability. In addition, this strategy could be an alternative to electrochemical cleaning which in spite of its ability to reactivate electrode surface, could damage the CFME as revealed in this work. Then, presently we have 2 originalities in the present study: the application of this strategy on CFME (for the first time) and at the molecule of MNP. Future works will consist in the application of this sensor to the analysis of the MNP in the presence of FT and others molecules phenol-likes, i.e. as *p*-nitrophenol and methylparathion.

ACKNOWLEDGMENTS

The authors would like to thank International Science Programme (ISP) for financial support of this work through the African Network of Electroanalytical Chemists (ANEC), Jean-Philippe BOUCHARA (director of GEIHP EA3142, Angers University, France) for acceptance of the internship of Fabrice BAKO from September to December 2016 in his research lab. in Angers (France) and Romain MALLET (SCIAM, Angers University, France) for its assistance to carry out the microscopy analysis.

References

1. D. Rodrigues, T. Carvalho, A. Sousa, V.S. Neto, P. Fehine and R. Nascimento, *Chromatogr. Res. Int.*, 2011 (2011) 1.
2. W. Geremedhin, M. Amare and S. Admassie, *Electrochim. Acta*, 87 (2013) 749.
3. Q. Zhang, Q. Sun, B. Hu, Q. Shen, G. Yang, X. Liang, X. Sun and F. Liu, *Food Chem.*, 106 (2008) 1278.
4. K. Seebunrueng, Y. Santaladchaiyakit and S. Srijaranai, *Chemosphere*, 103 (2014) 51.
5. FAO, (2013). faostat.fao.org (accessed January 28, 2014).

6. T. Kameya, M. Saito, T. Kondo, W. Toriumi, K. Fujie, T. Matsushita and H. Takanashi, *J. Water Environ. Technol.*, 10 (2012) 427.
7. A.N. Diaz, F.G. Sanchez, A. Aguilar, A.B.M. De Vicente and A. Bautista, *J. Food Compos. Anal.*, 42 (2015) 187.
8. T. Galeano-Díaz, A. Guiberteau-Cabanillas, A. Espinosa-Mansilla and M.D. López-Soto, *Anal. Chim. Acta*, 618 (2008) 131.
9. B. Bhushan, S.K. Samanta, A. Chauhan, A.K. Chakraborti and R.K. Jain, *Biochem. Biophys. Res. Commun.*, 275 (2000) 129.
10. R.A. Kanaly, A.I.S. Kim and H.G. Hur, *J. Agric. Food Chem.*, 53 (2005) 6426.
11. H. Katsumata, T. Okada, S. Kaneco, T. Suzuki and K. Ohta, *Ultrason. Sonochem.*, 17 (2010) 200.
12. C. Li, S. Taneda, A.K. Suzuki, C. Furuta, G. Watanabe and K. Taya, *Eur. J. Pharmacol.*, 543 (2006) 194.
13. D. De Souza, S.A.S. Machado, *Electroanalysis*, 18 (2006) 862.
14. A. Gahlaut, *Open J. Appl. Biosens.*, 1 (2012) 1.
15. M. Feng, H. Han, J. Zhang and H. Tachikawa, Electrochemical sensors based on carbon nanotubes, in *Electrochemical Sensors, Biosensors and Their Biomedical Applications*, Academic Press, (2008) San Diego, USA.
16. A. Kumaravel and M. Chandrasekaran, *J. Electroanal. Chem.*, 638 (2010) 231.
17. W. Yazhen, Q. Hongxin, H. Siqian and X. Junhui, *Sens. Actuators, B*, 147 (2010) 587.
18. S.N. Sinha, M.V.V. Rao, K. Vasudev and M. Odetokun, *Food Control*, 25 (2012) 636.
19. G.A.E. Mostafa, *Open Electrochem. J.*, 2 (2010) 22.
20. M. Pontié, G. Thouand, F. De Nardi, I. Tapsoba and S. Lherbette, *Electroanalysis*, 23 (2011) 1579.
21. Y.F.R. Bako, B. Kabore and I. Tapsoba, *Mater. Sci. Appl.*, 8 (2017) 798.
22. M. Sbaï, H. Essis-Tome, U. Gombert, T. Breton and M. Pontié, *Sens. Actuators, B*, 124 (2007) 368.
23. I. Tapsoba, S. Bourhis, T. Feng and M. Pontié, *Electroanalysis*, 21 (2009) 1167.
24. R.J. Forster and T.E. Keyes, *Handb. Electrochem.*, (2007) 155.
25. S. Szunerits and L. Thouin, *Handb. Electrochem.*, (2007) 391.
26. M. Ferreira, H. Varela, R.M. Torresi and G. Tremiliosi-Filho, *Electrochim. Acta*, 52 (2006) 434.
27. M.S. Ureta-Zañartu, P. Bustos, C. Berríos, M.C. Diez, M.L. Mora and C. Gutiérrez, *Electrochim. Acta*, 47 (2002) 2399.
28. M. Pontie, H. Lecture and F. Bedioui, *Sens. Actuators, B*, 56 (1999) 1.
29. A.J. Bard, L.R. Faulkner, E. Swain and C. Robey, *Electrochemical Methods: Fundamentals and Applications*, 2nd ed., John Wiley & Sons, (2001) New York, NY, USA.
30. D.P. Zhang, W.L. Wu, H.Y. Long, Y.C. Liu and Z.S. Yang, *Int. J. Mol. Sci.*, 9 (2008) 316.
31. H. Yin, Y. Zhou, S. Ai, X. Liu, L. Zhu and L. Lu, *Microchim. Acta*, 169 (2010) 87.
32. X. Yang, J. Kirsch, J. Fergus and A. Simonian, *Electrochim. Acta*, 94 (2013) 259.
33. N.B. Tahar and A. Savall, *Electrochim. Acta*, 55 (2009) 465.
34. P. Krawczyk and J.M. Skowroński, *Electrochim. Acta*, 79 (2012) 202.
35. M.S. Ureta-Zañartu, C. Berríos, J. Pavez, J. Zagal, C. Gutiérrez and J.F. Marco, *J. Electroanal. Chem.*, 553 (2003) 147.
36. J. Obirai, F. Bedioui and T. Nyokong, *J. Electroanal. Chem.*, 576 (2005) 323.
37. S.F. Mbokou, M. Pontié, J. Bouchara, F. Merlin, M. Tchieno, E. Njanja, A. Mogni, P.Y. Pontalier and I.K. Tonle, *Int. J. Electrochem.*, 2016 (2016).